Available online at www.sciencedirect.com
ScienceDirect
Ceramics International 37 (2011) 835–841
CERAMICS INTERNATIONAL
www.elsevier.com/locate/ceramint

Influence of chemical composition on sintering ability of ZTA ceramics consolidated from freeze dried granules

Ibram Ganesh [a,*], G. Sundararajan [a], S.M. Olhero [b], J.M.F. Ferreira [b]

[a] Centre for Advanced Ceramics, International Advanced Research Centre for Powder Metallurgy and New Materials (ARCI), Hyderabad 500005, A.P., India
[b] Department of Ceramics and Glass Engineering, CICECO, University of Aveiro, Aveiro P-3810193, Portugal

Received 9 April 2010; received in revised form 6 October 2010; accepted 14 October 2010
Available online 18 November 2010

Abstract

Dense zirconia-toughened alumina (ZTA) ceramic composites with ZrO_2 = 0, 5, 10, 15, 20, 30, 60 and 100 wt.% have been prepared by sintering green compacts obtained by dry powder pressing of freeze dried granules consisting of α-alumina and a yttria partially stabilized zirconia (YPSZ) at various temperatures ranging from 1450 to 1650 °C for 1–2 h. The characteristics of sintered products were determined by X-ray diffraction (XRD), scanning electron microscopy (SEM), Archimedes principle, Vickers indentation method and by 3-point bend test. Characterization results revealed that adding YPSZ increased the 3-point bend (flexural) strength, fracture toughness and homogeneity of the microstructure, but slightly decreased the hardness and the sintering ability of alumina. A 20 wt.% YPSZ was sufficient to increase the fracture toughness and flexural strength of specimens sintered for 2 h at 1600 °C from 2.5 to 4.6 MPa $m^{1/2}$ and 150 to 400 MPa, respectively. The XRD results revealed that there is no solid-solution formation between zirconia and alumina constituents of ZTA ceramic composites upon sintering.

Keywords: C. Hardness; C. Strength; ZTA ceramics; Freeze granulation; Fracture toughness

1. Introduction

Considering the vast number of their potential applications, and the strong influence of chemical composition on their final properties and performance in a given application, it was suggested to investigate the effect of chemical composition on sintering ability and sintered properties of ZTA ceramic composites over a wider chemical composition range [1–16]. Furthermore, the properties of ZTA ceramic composites consolidated by dry powder pressing of freeze dried granules have not yet been studied so far, despite the superior properties of ceramics prepared from freeze dried granules in comparison to those prepared by spray drying and other conventional techniques. In view of the above, a systematic study was undertaken in this investigation to prepare dense zirconia–alumina ceramic composites with ZrO_2 = 0, 5, 10, 15, 20, 30, 60, and 100 wt.% consolidated by dry-powder pressing of freeze dried granules, followed by sintering for 1–2 h at 1450–1650 °C. The sintered ceramic composites were thoroughly characterized by various techniques and the obtained results are presented and discussed in this paper.

2. Experimental procedure

2.1. Powder processing

An alumina powder (CT-3000SG, Alcoa-Chemie GmbH, Germany, with an average particle size, D_{50} = 0.8 μm) and a yttria partially stabilized zirconia (YPSZ) powder (Tosoh-Zirconia, TZ-3YS, Yamaguchi, Japan, D_{50} = 0.43 μm) were used in this study as raw materials. Eight zirconia-toughened alumina (ZTA) compositions were formulated as summarised in Table 1. For easy identification purposes, codes are given to these compositions. In the codes, ZTA stands for zirconia-toughened alumina, and the numbers 0–100 indicate the weight percent of zirconia in the composite. All the powder compositions were dispersed in double distilled water to obtain stable suspensions with 50 vol.% solids loading using

* Corresponding author. Tel.: +91 040 24442699.
E-mail addresses: ibramganesh@arci.res.in, ibram_ganesh@yahoo.com (I. Ganesh).

0272-8842/$36.00
doi:10.1016/j.ceramint.2010.10.027

Table 1
Precursor compositions and green properties of pellets consolidated by die-pressing of freeze dried granules.

Sample[a]	Al_2O_3 (wt.%)	ZrO_2 (wt.%)	Green density, GD (g/cm^3)	Relative density, RD[b] (%)	Theoretical density, TD[c] (g/cm^3)
ZTA-0	100	0	2.271	57.20	3.97
ZTA-5	95	5	2.289	56.16	4.076
ZTA-10	90	10	2.291	54.77	4.183
ZTA-15	85	15	2.294	53.48	4.289
ZTA-20	80	20	2.326	52.91	4.396
ZTA-30	70	30	2.331	50.57	4.609
ZTA-60	60	40	2.592	49.39	5.248
ZTA-100	0	100	2.968	48.65	6.101

[a] In the sample codes, ZTA stands for zirconia-toughened alumina and the numbers 0–100 represent the zirconia weight percent in the composition.
[b] Relative density, RD = [GD/TD] × 100.
[c] The theoretical density of green compacts was estimated based on the rule of mixtures from the theoretical densities of alumina (3.97 g/cm^3) and zirconia (6.101 g/cm^3).

Dolapix CE 64 (an aqueous solution of a polycarboxylic acid without alkalis, Zschimmer and Schwarz, Chemnitztalstrasse, Germany) as dispersant at the ratio of 0.4 wt.% (based on powder basis) [15,16]. The suspensions were ball milled for 24 h in the polypropylene bottles using alumina balls (the charge to balls ratio was 1:3). After degassing by vacuum pumping, these suspensions were diluted to 35 vol.% by adding the required amount of distilled water and 3 wt.% of an emulsion binder, Duramax D1000 (Rohm and Haas, Lauterbourg, France) on powder weight basis. It is well known that deagglomeration of powder particles in a suspension is easier at moderate-high solids loading in comparison to diluted suspensions. On the other hand, the concentrated suspensions tend to exhibit shear thickening characteristics when submitted to high shear rates as those prevailing upon passing through a narrow (0.7 mm diameter) spraying nozzle. Because of these reasons, the suspensions were diluted prior to freeze granulation by spraying into liquid nitrogen (−196 °C) (Power Pro freeze granulator LS-2, Gothenburg, Sweden). The resultant granules were then dried at −49 °C under a pressure 1×10^{-3} Torr in a freeze drying system (Labconco, LYPH Lock 4.5, Kansas City, USA) for several days. A digital photograph of freeze dried granules formed out of ZTA-30 composition is depicted in Fig. 1. The fully dried (at 90 °C for 24 h in an electric oven) granules were then uni-axially pressed in a metal die by applying a pressure of 200 MPa to obtain pellets of about 20 mm diameter and 8–10 mm height [15,16].

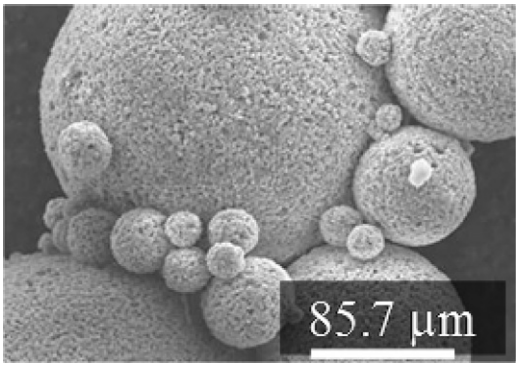

Fig. 1. ZTA-30 granules made by freeze granulation method.

2.2. Characterization techniques

Bulk density, apparent porosity and water absorption capacity of sintered ZTA ceramics were measured in aqueous media according to Archimedes principle (ASTM C372) using Mettler balance and the attachment (AG 245, Mettler Toledo, Switzerland). In average, three density measurements were performed for each sample in this study (±0.01 error) [15–18]. XRD patterns were recorded on a Rigaku machine (Tokyo, Japan) using diffracted beam mono-chromated Cu K_α (0.15406 nm) radiation source [19]. Crystalline phases were identified by comparison with PDF-4 reference data from International Centre for Diffraction Data (ICDD) [20]. Microstructures of dense ZTA ceramics were examined by SEM (Hitachi S-4100, Tokyo, Japan) with an energy dispersive analysis with X-rays (Sigma 3.42 Quaser, Kevex, USA) for qualitative and quantitative analysis. Prior to analysis, all the samples were mounted on araldite platform, polished, thermally etched (at 1500 °C for 10 min) and coated with carbon for conductivity. The fracture toughness (K_{Ic}) values were calculated on the basis of the indentation method ($K_{Ic} = Ha^{1/2} \times 0.203(C/a)^{-3/2}$), where $2a$ represents Vickers indent diagonal length, C the resulted crack length and H is a Vickers hardness (H_V = kg/mm^2 = 10 MPa) [21]. Five to six samples were examined per case; in order to check the reproducibility of results and all the 5 readings were averaged out [15,16]. Hardness was determined by applying a Vickers indenter and calculated as $H = P/2d^2$, d being the half-diagonal indentation impression and P the indentation load (10 kg). The flexural strength was measured using the 3-point bend test (JIS-R1601) conducted on a universal testing machine. The required hardness and the crack and diagonal length data was collected using a micro-hardness tester (Leitz Wetzler, Germany) by holding the indenter tip (with 137°) under 10 kg load for 20 s on the polished surface of the sample.

3. Results and discussion

The precursor compositions tested and the values of apparent green density (GD), relative density (RD), and theoretical density (TD) based on the rule of mixtures from the

theoretical densities of alumina (3.97 g/cm^3) and YPSZ (6.101 g/cm^3) of green bodies are presented in Table 1. The percentage of relative density of green bodies is given by RD = [GD/TD] × 100. The gradual increase of zirconia in the precursor compositions resulted in an overall increase of green density due to the higher theoretical density of this oxide. But the increment in density was not proportional to the amount of ZrO_2, resulting in a gradual decrease of relative density, despite the constant consolidation pressure (200 MPa) and the fixed amount of emulsion binder (3 wt.% on powder weight basis) used. The decrease of relative density with increasing added amounts of YPSZ powder can be attributed to the poor packing ability of starting powder mixtures enriched in the finer component YPSZ (D_{50} = 0.43 μm), in comparison to D_{50} = 0.8 μm for alumina [22].

Furthermore, the relative density values measured for dry powder pressed compacts are lower in comparison to those reported in the literature for similar ceramic composites consolidated by different colloidal shaping methods [15,16]. The ZTA-30 and ZTA-60 green bodies consolidated by slip casting, hydrolysis assisted solidification, aqueous gelcasting and hydrolysis induced aqueous gelcasting routes exhibited relative densities of 60.75, 52.07, 59.88 and 52.07%, and of 60.97, 54.11, 56.97 and 54.21%, respectively. However, the ZTA-30 and ZTA-60 green pellets prepared by dry powder pressing exhibited relative densities of only 50.57% and 49.39%, respectively [15,16]. These results clearly suggest that the compaction degree achieved in green ZTA pellets strongly depends on the consolidation process used. Accordingly, higher relative densities are obtained for green bodies consolidated by colloidal processing routes that enable to control the inter particle forces in the suspensions. This explains why green densities of pellets consolidated by colloidal processes increased when passing from ZTA-30 to ZTA-60 [15,16], contrarily to the trend observed in the present work for green bodies consolidated by dry powder pressing.

The XRD patterns of ZTA ceramics consolidated by dry powder pressing of freeze dried granules followed by sintering for 2 h at 1600 °C are presented in Fig. 2. The XRD data of standard ICDD files for corundum (α-Al_2O_3, No.: 00-046-1212), monoclinic zirconia (*m*-ZrO_2, No.: 00-037-1484) and zirconia–yttria compound {$[(ZrO_2)_{0.91}(Y_2O_3)_{0.09}]_{0.917}$, No.: 01-083-0113} are also presented in Fig. 2 for an easy comparison purposes. The diffraction lines primarily due to corundum and $[(ZrO_2)_{0.91}(Y_2O_3)_{0.09}]_{0.917}$ phases are seen in these spectra. None of the lines belonging to compounds formed out of constituent oxides are seen. These results indicate that there is no compound formation between zirconia and alumina during sintering [15,16].

Relative density values of ZTA-0 to ZTA-100 composites sintered for 1–2 h in the range of 1450–1650 °C are presented in Fig. 3. The percentage of relative density of sintered bodies was calculated as RD = [BD/TD] × 100, where BD stands for bulk density [9,10]. As expected, RD increased with increasing sintering temperature and holding time, achieving almost full density for (ZTA-100) sample sintered for 2 h at 1600 °C. The measured RD values for alumina (ZTA-0) and zirconia-toughened alumina (ZTA-5 to ZTA-60) composites were about 98%. The lowest RD value of about 94% was measured for ZTA-60. These relative density values increased with the sintering temperature of up to 1600 °C and then tended to slightly decrease for higher temperatures due to pore

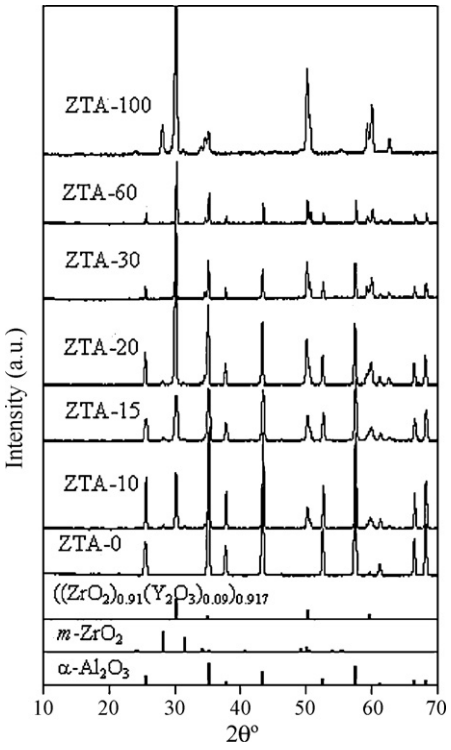

Fig. 2. XRD of ZTA-0 to ZTA-100 sintered for 2 h at 1600 °C. α-Al_2O_3 (ICDD File No.: 00-046-1212); *m*-ZrO_2 (ICDD File No.: 00-037-1484); $[(ZrO_2)_{0.91}(Y_2O_3)_{0.09}]_{0.917}$ (ICDD File No.: 01-083-0113).

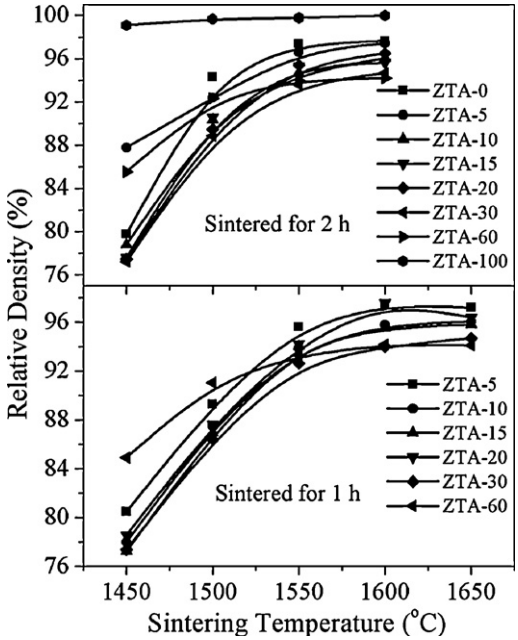

Fig. 3. Relative density of ZTA-0 to ZTA-100 sintered for 1–2 h at 1450–1650 °C. The percentage of relative density was calculated as RD = [BD/TD] × 100, where BD stands for bulk density.

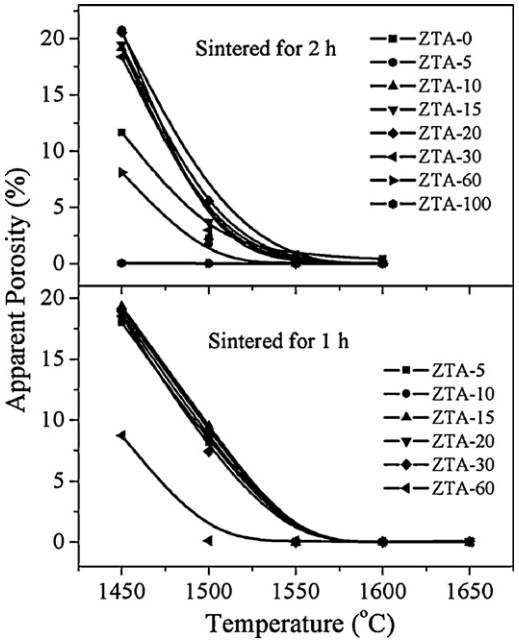

Fig. 4. Apparent porosity of ZTA-0 to ZTA-100 ceramics sintered for 1–2 h at 1450–1650 °C.

coalescence [23]. This increase is better noticed in the case of pure alumina (ZTA-0) in comparison to ZTA-5 to ZTA-60 ceramic composites. These results suggest that the TZ-3YS powder possesses excellent sintering ability when compared with pure alumina. This is could be due to its finer average particle size (D_{50} = 0.43 μm) than that of alumina (D_{50} = 0.8 μm) powder. These results further suggest that despite its finer average particle size, YPSZ hampers the sintering ability of alumina. Contrary to this, YPSZ addition has enhanced the sintering ability of certain powders such as,

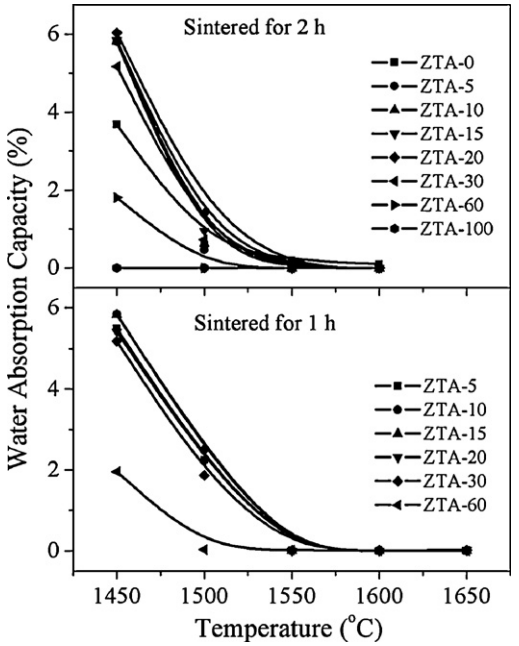

Fig. 5. Water absorption capacity of ZTA-0 to ZTA-100 ceramics sintered for 1–2 h at 1450–1650 °C.

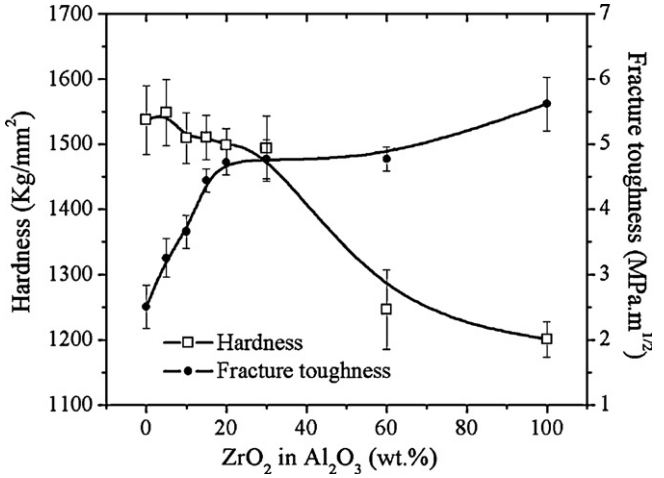

Fig. 6. Hardness and fracture toughness of ZTA-0 to ZTA-100 ceramics sintered for 2 h at 1600 °C.

$MgAl_2O_4$ spinel, composites of MgO/$MgAl_2O_4$ spinel, etc. [23–26]. According to Yamaguchi et al. [25], when ZrO_2 (m.p. ~2623 °C) is added to MgO (m.p. ~2800 °C)/$MgAl_2O_4$ spinel (m.p. ~2135 °C) composite, Zr^{4+} goes into MgO lattice since Zr^{4+} and Mg^{2+} have the same ionic radii of 0.72 Å, therefore forming a solid solution of ZrO_2–MgO and creating magnesium ion vacancies in MgO crystals. These vacancies accelerate the diffusion of O^{2-} ions to form dense products at >1500 °C. Furthermore, ZrO_2 is also known to accelerate the oxygen ion diffusion thereby the sintering ability of certain ceramic powders [25]. However, the same mechanism seems to be not applicable in the present case of alumina due to the large difference in ionic radii of Zr^{4+} (0.72 Å) and Al^{3+} (0.52 Å). These results suggest that 1600 °C is the optimal sintering temperature for densifying the ZTA composites prepared in this study. A good balance between the densification level and the coarsening of the sintered microstructure has to be found in order to maximise the retention levels of meta-stable phase and strengths in zirconia based materials [24].

The evolution of apparent porosity and water absorption capacity values of ZTA-0 to ZTA-100 ceramics sintered for 1–

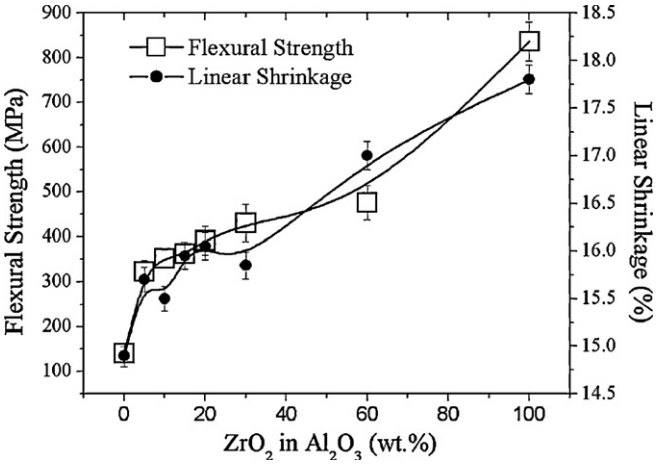

Fig. 7. Flexural strength and linear shrinkage of ZTA-0 to ZTA-100 ceramics sintered for 2 h at 1600 °C.

2 h at 1450–1650 °C presented in Figs. 4 and 5, respectively show similar trends with varying sintering temperature and holding time. The highest apparent porosity (∼22%) and water absorption capacity (∼6%) values were measured for the composites sintered at 1450 °C, decreasing to almost zero after sintering at 1600 °C irrespective of chemical composition and holding time. For pure YPSZ (ZTA-100), impervious ceramics could be obtained after sintering for 2 h even at 1450 °C. The results of apparent porosity and water absorption capacity are consistent with the measured relative sintered densities.

The values of hardness and fracture toughness of ZTA-0 to ZTA-100 ceramics sintered for 2 h at 1600 °C are plotted in Fig. 6 and their corresponding flexural strength and percentage of linear shrinkage values are presented in Fig. 7 as a function of zirconia content. A slight decrease in hardness from 1540 to 1500 kg/mm^2 is observed in the range of 0–30 wt.% zirconia, followed by a more accentuated decrease to 1240 kg/mm^2 for 60 wt.% YPSZ. The pure YPSZ (ZTA-100) exhibited a lowest value of about 1200 kg/mm^2. In contrast to hardness values, there is an improvement in the fracture toughness from 2.5 to

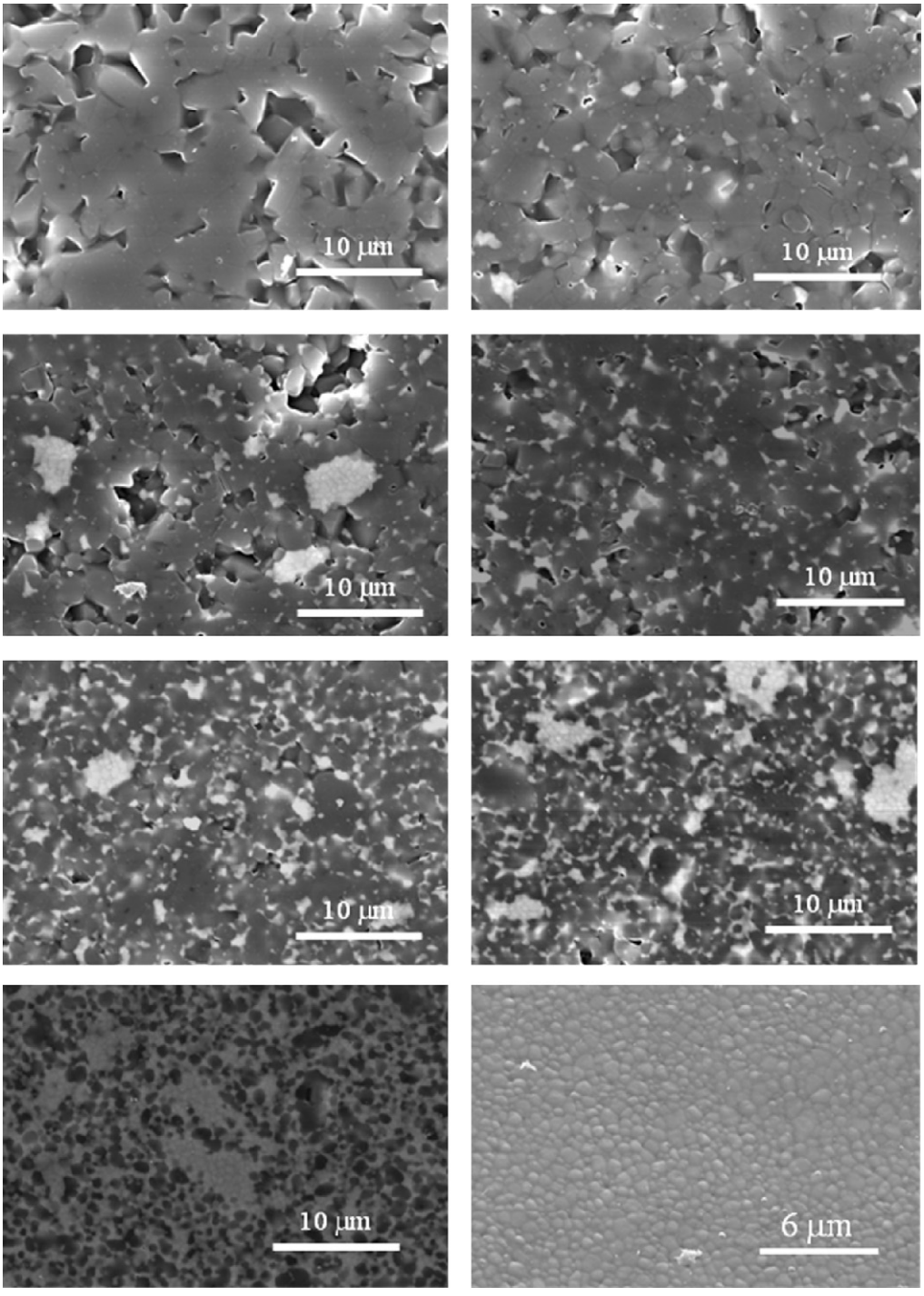

Fig. 8. SEM micrographs of ZTA-0 to ZTA-100 ceramics sintered for 2 h at 1600 °C.

4.6 MPa $m^{1/2}$ when zirconia concentration was increased from 0 to 20 wt.%, followed by a further increase to 4.8 MPa $m^{1/2}$ when the proportion of this oxide was increased to 60 wt.%. The pure YPSZ exhibited a fracture toughness of about 5.66 MPa $m^{1/2}$ after sintering for 2 h at 1600 °C.

Interestingly, both percentage linear shrinkage and flexural strength of ceramics sintered for 2 h at 1600 °C exhibited similar increasing trends with as a function of added amounts of zirconia (Fig. 7). These variations are consistent with the lower relative green densities of zirconia-rich compacts, its finer particle size, and the intrinsic mechanical properties of zirconia. The flexural strength increased from 150 MPa (ZTA-0) to about 400 MPa (ZTA-20), 430 MPa (ZTA-30), and 465 MPa (ZTA-60). The pure YPSZ sintered for 2 h at 1600 °C exhibited a flexural strength of about 840 MPa. The improved flexural strength and fracture toughness with the increase of zirconia concentration in ZTA composite can be attributed to the four toughening mechanisms identified in these composites, which are related to the volume expansion and shear strain associated with the t → m transformation of zirconia [6–16,23]. The first is the stress-induced transformation toughening mechanism. Application of an external tensile stress around a crack tip introduces phase transformation (t → m), accompanied by volume expansion (≈4%) and shear strain (≈6%) resulting in a compressive stress, which reduces propagation of crack and eventually stops it. This necessitates extra work for further crack propagation. In the micro crack toughening mechanism, the micro cracks (either residual or stress induced), by their ability to extend in the stress field of a propagating crack, can absorb the fracture energy, increasing the material toughness. Cracks can also be deflected by localized stress fields which are developed as a result of phase transformation, or by fracture of second particles, thus enhancing toughness. Finally, the compressive surface stress, which is a resultant of the compressive volume expansion and shear strain associated with t → m transformation on the surface, is an apparent toughening factor for ZTA ceramics [6–16,23].

The evolution of sintered (for 2 h at 1600 °C) microstructure of ZTA ceramics with increasing zirconia contents can be seen in Fig. 8. The white portion in these micrographs is zirconia and the dark portion is either alumina or porosity. As expected, there is an increase in the white portion with the increasing zirconia contents. Interestingly, the homogeneity in distribution of zirconia and alumina portions in these composites is enhanced with increasing proportions of zirconia. The amount of open porosity seems to decrease with increasing contents of zirconia in line with the linear shrinkage data (Fig. 5), but in apparent contrast with relative density data (Fig. 3) [15,16].

4. Conclusions

The following conclusions can be drawn from the above study:

(1) Dense ZTA ceramics with 0, 5, 10, 15, 20, 30, 60 and 100 wt.% yttria partially stabilized zirconia (YPSZ) could be prepared by sintering (1–2 h, 1600 °C) green compacts consolidated by dry pressing of freeze dried granules.
(2) The flexural strength and fracture toughness increases and the sintering ability decreases with the increasing concentration of YPSZ in ZTA ceramics.
(3) The degree of homogeneity in the microstructure of sintered ZTA ceramics increases with increasing concentration of YPSZ.
(4) Due to the large difference between the ionic radii of Zr^{4+} (0.72 Å) and Al^{3+} (0.52 Å), ZrO_2 and Al_2O_3 do not react to form any new compound during sintering of ZTA ceramics.

Acknowledgements

IG thanks SERC-DST (Government of India) for the awarded BOYSCAST fellowship (SR/BY/E-04/06). The financial support of CICECO is also acknowledged.

References

[1] W.H. Gitzen, Alumina as a Ceramic Material, Special Publication No. 4, American Ceramic Society, 735 Ceramic Place, Westerville, Ohio 43081, 1970, , and references therein.
[2] D.B. Binns, The testing of alumina ceramics for engineering applications, J. Br. Ceram. Soc. 2 (1965) 294–308.
[3] G. Willmann, Ceramic femoral head for total hip arthroplasty, Adv. Eng. Mater. 2 (3) (2000) 114–121.
[4] G. Willmann, Development in medical-grade alumina during the past two decades, J. Mater. Proc. Technol. 56 (1996) 168–176.
[5] B. Liang, C. Ding, H. Liao, C. Coddet, Study on structural evolution of nano-structured 3 mol% yttria stabilized zirconia coatings during low temperature ageing, J. Eur. Ceram. Soc. 29 (11) (2009) 2267–2273.
[6] J.B. Huh, S.E. Eckert, S.M. Ko, Y.G. Choi, Heat transfer to the implant-bone interface during preparation of a zirconia/alumina abutment, J. Oral Maxillofac. Implants 24 (4) (2009) 679–683.
[7] B. Yuzugullu, A.M. Avci, The implant-abutment interface of alumina and zirconia abutments, Clin. Implant Dent. Relat. Res. 10 (2) (2008) 113–121.
[8] N. Claussen, Fracture toughness of Al_2O_3 with an un-stabilized ZrO_2 dispersed phase, J. Am. Ceram. Soc. 59 (1976) 49–51.
[9] J. Wang, R. Stevens, Review: zirconia-toughened alumina (ZTA) ceramics, J. Mater. Sci. 24 (10) (1989) 3421–3440.
[10] G. Magnani, A. Brillante, Effect of the composition and sintering process on mechanical properties and residual stresses in zirconia–alumina composites, J. Eur. Ceram. Soc. 25 (2005) 3383–3392.
[11] D. Casellas, M.M. Nagl, L. Llanes, M. Anglada, Fracture toughness of alumina and ZTA ceramics: micro-structural coarsening effects, J. Mater. Proce. Tech. 143–144 (2003) 148–152.
[12] W.H. Tuan, R.Z. Chen, T.C. Wang, C.H. Cheng, P.S. Kuo, Mechanical properties of Al_2O_3/ZrO_2 composites, J. Eur. Ceram. Soc. 22 (16) (2002) 2827–2833.
[13] Y. Shin, Y. Rhee, S. Kang, Experimental evaluation of toughening mechanism in alumina–zirconia composites, J. Am. Ceram. Soc. 82 (5) (1999) 1229–1232.
[14] R.H.J. Hannink, P.M. Kelly, B.C. Muddle, Transformation toughening in zirconia-containing ceramics, J. Am. Ceram. Soc. 83 (3) (2000) 461–487.
[15] I. Ganesh, S.M. Olhero, P.M.C. Torres, F.J. Alves, J.M.F. Ferreira, Hydrolysis induced aqueous gelcasting for near-net shaping of ZTA ceramic composites, J. Eur. Ceram. Soc. 29 (2009) 1393–1401.
[16] S.M. Olhero, I. Ganesh, P.M.C. Torres, F.J. Alves, J.M.F. Ferreira, An aqueous colloidal processing of ZTA composites, J. Am. Ceram. Soc. 92 (1) (2009) 9–16.

[17] I. Ganesh, S.M. Olhero, A.H. Rebelo, J.M.F. Ferreira, Formation and densification behaviour of $MgAl_2O_4$ spinel: the influence of processing parameters, J. Am. Ceram. Soc. 91 (6) (2008) 1905–1911.
[18] I. Ganesh, K.A. Teja, N. Thiyagarajan, R. Johnson, B.M. Reddy, Formation and densification behaviour of magnesium aluminate spinel: the influence of CaO and moisture in the precursors, J. Am. Ceram. Soc. 88 (10) (2005) 2752–2761.
[19] B.D. Cullity, Elements of XRD, 2nd ed., Addison-Wesley, Reading, MA, 1978.
[20] H.P. Klug, L.E. Alexander, X-ray diffraction procedure for polycrystalline and amorphous materials, J. Appl. Crystallogr. 8 (1975) 573.
[21] G.R. Anstis, P. Chantikul, B.R. Lawn, D.B. Marshall, A critical evaluation of indentation techniques for measuring fracture toughness: I direct crack measurements, J. Am. Ceram. Soc. 64 (1981) 533–538.
[22] G. Tari, J.M.F. Ferreira, A.T. Fonseca, O. Lyckfeld, Influence of particle size distribution on colloidal processing of alumina, J. Eur. Ceram. Soc. 18 (1998) 249–253.
[23] T. Suzuki, K. Itatani, M. Aizawa, F. Scott Howell, A. Kishioka, Sinterability of spinel ($MgAl_2O_4$)-zirconia composite powder prepared by double nozzle ultrasonic spray pyrolysis, J. Eur. Ceram. Soc. 16 (1996) 1171–1178.
[24] I. Ganesh, J.M.F. Ferreira, Synthesis and characterization of $MgAl_2O_4$-ZrO_2 composites, Ceram. Int. 35 (2009) 259–264.
[25] G. Yamaguchi, M. Nakano, R. Ychimura, Yogyo-Kyokai-shi 79 (1971) 140–145.
[26] H.W. Walter, W.S. Thomas, Chemical preparation of zirconium-aluminum-magnesium oxide composites, US patent No. 4880757, Nov. 14th, 1989.